

Magneto-optic surface plasmon resonance optimum layers: Simulations for biological relevant refractive index changes

Kerstin Kämpf, Sebastian Kübler, Friedrich Wilhelm Herberg, and Arno Ehresmann

Citation: [Journal of Applied Physics](#) **112**, 034505 (2012); doi: 10.1063/1.4742130

View online: <http://dx.doi.org/10.1063/1.4742130>

View Table of Contents: <http://scitation.aip.org/content/aip/journal/jap/112/3?ver=pdfcov>

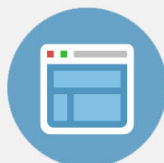
Published by the [AIP Publishing](#)

Advertisement:



Re-register for Table of Content Alerts

Create a profile.



Sign up today!



Magneto-optic surface plasmon resonance optimum layers: Simulations for biological relevant refractive index changes

Kerstin Kämpf,¹ Sebastian Kübler,^{1,a)} Friedrich Wilhelm Herberg,² and Arno Ehresmann¹

¹*Institute of Physics and Center for Interdisciplinary Nanostructure Science and Technology (CINSA-T), University of Kassel, Heinrich-Plett-Str.40, 34132 Kassel, Germany*

²*Institute of Biology and Center for Interdisciplinary Nanostructure Science and Technology (CINSA-T), University of Kassel, Heinrich-Plett-Str.40, 34132 Kassel, Germany*

(Received 9 May 2012; accepted 5 July 2012; published online 6 August 2012)

The transfer matrix method is used to simulate the magneto-optic surface plasmon resonance (MOSPR) of Au/Co/Au trilayer systems focused on the magneto-optic activity in transverse configuration. The results show a strong thickness dependence of the normalized difference of reflectivity at opposite directions of the magnetization (δ -signal) and a strong change of the δ -signal with the refractive index n of the biologically active layer. Within a range of the refractive index typically covered by a commercial SPR biosensor ($n = 1.33 - 1.40$), the magnitude of the δ -signal of an Au(10.75 nm)/Co(6 nm)/Au(20.25 nm) trilayer decreases from small to large n by a factor > 63 . This finding demonstrates that the enhanced sensitivity of an MOSPR biosensor can be exploited only by defined thicknesses of the metal layers for distinct refractive index regions. © 2012 American Institute of Physics. [<http://dx.doi.org/10.1063/1.4742130>]

I. INTRODUCTION

The surface plasmon resonance (SPR) effect is employed as a tool for label-free investigation of interactions between biomolecules since the early 1990s.¹ A surface plasmon resonance is a surface charge density wave in a metal layer (*e.g.*, Au, Ag), excited by light and propagating along the interface between a metal and a dielectric. For biosensing, the dielectric is part of a fluid cell and contains usually a matrix where one binding partner is immobilized (“ligand”) and the interaction with other biomolecules (“analyte”), passing through the fluid cell may be monitored. The evanescent field connected with the charge density wave penetrates into the fluid cell and is used for sensing applications. A typical set-up of such a biosensor is displayed in Fig. 1 in the Kretschmann geometry.² In such a set-up the back side of the metal layer (here: an Au/Co/Au trilayer for magneto-optic surface plasmon resonance (MOSPR)) is functionalized as a biologically active matrix. In the Kretschmann geometry [Fig. 1] the excitation of the SPR takes place, if the angle of incidence θ matches the resonance condition,

$$k_{SP,x} = \frac{\omega}{c} \left(\frac{\epsilon_m(\omega)\epsilon_d(\omega)}{\epsilon_m(\omega) + \epsilon_d(\omega)} \right)^{1/2} = \frac{\omega}{c} \sqrt{\epsilon_p} \sin \theta = k_{L,x} \quad (1)$$

in which ϵ_m is the permittivity of the metal, ϵ_d the permittivity of the dielectric (matrix with bound analyte), and ϵ_p the permittivity of the glass prism. $k_{L,x}$ is the projection of the wave vector of the p -polarized incident light along the metal surface and $k_{SP,x}$ the wave vector of the associated surface plasmon [Fig. 1]. When the resonance condition for excitation of a surface plasmon is met, a drop of reflected intensity is observed. If binding occurs the permittivity of the dielectric in front of the metal and therefore $k_{SP,x}$ is changed.

As the permittivity ϵ_d and hence the resonance angle θ depends on the concentration of biomolecules bound to the ligand matrix, the angle of the minimum intensity can be used to quantify the binding affinities and binding kinetics of biomolecules. However, for the characterization of an interacting pair of biomolecules using a low molecular weight molecule (< 500 g/mol) as an analyte, the sensitivity of SPR biosensors is in many cases not sufficient, since the refractive index n is approximately proportional to the mass of the solute biomolecules.³ In the past years a number of approaches have shown to improve the sensitivity, *e.g.*, by introducing a ZnO-Layer⁴ or by using localized surface plasmon resonance (LSPR).^{5,6} One of the recent approaches is the combination of SPR with the magneto-optic Kerr effect (MOKE)^{7,8} also combined with LSPR.⁹⁻¹³

The MOKE is a change in reflected intensity or polarization of a linearly polarized ray of light after interaction with magnetic material. The strength of the MOKE depends on the magnetization of the material and the magnitude of the electromagnetic field. The latter property is exploited for the combination of the MOKE and the SPR to the MOSPR: As the excitation of a surface plasmon at the interface of a metal and a dielectric is accompanied by a high electromagnetic field propagating along the metal surface facing the dielectric and decaying exponentially to both sides, this electromagnetic field enhances the MOKE and in turn may also enhance the sensitivity of the MOSPR effect compared to the normal SPR effect. Sepúlveda *et al.*^{8,14} reported for example an up to four times higher sensitivity of a MOSPR based sensor compared to standard SPR sensors and suggested still higher sensitivities by optimized set-ups.

In a MOSPR set-up, the gold layer of an SPR set-up is combined with a magnetic thin film or multilayer. Due to the strong absorption of magnetic layers the quality of the plasmon decreases. Therefore a delicate trade off between thin film thicknesses and magnetic layer composition is essential.

^{a)}Electronic mail: kuebler@uni-kassel.de.

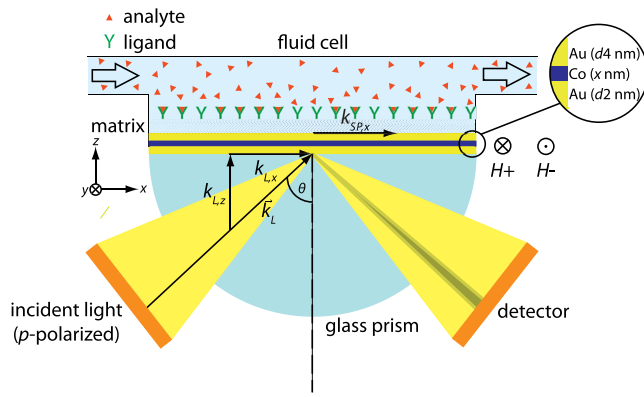


FIG. 1. Principle of an SPR/MOSPR biosensor. An Au layer (SPR) or an Au/Co/Au trilayer (MOSPR) is deposited on the backside of a glass prism facing a fluid cell. To the upper Au layer a chemically functionalized matrix is attached, containing the ligand molecules. Through the fluid cell, a solution containing the analyte is conducted. If p -polarized light with wave vector k_L is reflected at the backside of the metal layer system a surface plasmon (wave vector $k_{SP,x}$) can be excited when $k_{L,x} = k_{SP,x}$, detected by a minimum in reflected light. $k_{SP,x}$ and for this reason the resonance angle θ depends on the refractive index in front of the uppermost Au layer. θ therefore depends on the amount of analyte bound to the matrix/ligands. For MOSPR, the reflectivity depends on the magnetization of the Co layer due to the transverse magneto-optic Kerr effect.

It turned out, that cobalt sandwiched in an Au/Co/Au trilayer system is well suited for MOSPR in transverse geometry.^{15–17} There have been several theoretical approaches to find the layer composition leading to the highest MOSPR signal.^{8,16,18,19} However, these calculations have only been performed for minor or no changes of the refractive index on the back side of the metal layer system, *i.e.*, in the biologically active matrix. Also the change of the plasmon quality and the magneto-optic response have not been investigated for refractive index changes of the matrix in the range usually covered by commercial biosensors ($n = 1.33–1.40$).

In the present paper, results of calculations are presented demonstrating the strong dependence of the MOSPR effect in an Au/Co/Au trilayer system on the refractive index of the dielectric. It will be shown that in contrast to an SPR biosensor the optimum thickness combination of the metallic layers depends on the dielectric matrix, therefore on the biological system to be investigated. This enables a specific design of the layer thicknesses to the special needs of the analyte to be detected. We further demonstrate that the enhancement of the sensitivity in the MOSPR biosensor is driven by an enhanced change in signal per angle rather than an increased angular dispersion per refractive index.

II. METHODS

The reflectivity of Au/Co/Au three layer systems illuminated by light with $\lambda = 635$ nm from the front side through a half cylindrical glass (BK7, $n = 1.515$) prism in Kretschmann geometry has been calculated by the matrix formalism for magneto-optical multilayer systems of Zak *et al.*^{20,21} The magnetic permeability μ was considered to be $\mu = 1$. The permittivity of the metals was taken from¹⁴: $\epsilon(\text{Au}) = -11.00 + i1.98$ and $\epsilon(\text{Co}) = -11.43 + i18.15$. The magneto-optical properties of cobalt are represented by the so called Voigt

constant Q , which was considered as $Q = 0.043 + i0.007$.²² The material of the dielectric layer was first considered to be air $\epsilon = 1$ and was then replaced by water $\epsilon = 1.77$ ($n = 1.33$). The conditions of a biosensor have been simulated by dividing the dielectric into a 100 nm thick zone on top of the gold layer with varying the refractive index representing the ligand matrix of a biosensor and into a second zone, the bulk dielectric (water) with $n = 1.33$.

The small change in reflectivity caused by the MOSPR effect, the normalized difference of the reflectivity at opposite directions of the magnetization $R(H+)$ and $R(H-)$, pointing into the transverse direction is measured in the experiments described in literature.^{7,8,14,19} Accordingly we calculated the MOSPR difference signal δ ,

$$\delta = \frac{R(H+) - R(H-)}{R(0)}, \quad (2)$$

where $R(0)$ is the reflectivity without an magnetization of the Co layer perpendicular to the plane of incidence. In the following, we will use the brief expression Au($d2$ nm)/Co(x nm)/Au($d4$ nm) to describe the composition of the investigated multilayer system. The order of the layers is given starting from the glass prism towards the dielectric medium. The definition of the coordinate system and the definition of the relevant quantities are displayed in Fig. 1.

III. RESULTS AND DISCUSSION

A. Optimum layers for air

In a first set of simulations and as a verification of our calculations, we investigated the thickness dependence of the maximum MOSPR signal δ with the dielectric air. The thicknesses of both gold layers have been varied between 0 and 50 nm at constant cobalt thicknesses of 4 and 6 nm [Fig. 2]. The red bands mark those combinations of thicknesses of the two gold layers, at which the MOSPR signal for the given cobalt thickness is high ($\delta > 0.5$). Outside these narrow areas, the MOSPR signal is very low. An increase of the cobalt thickness leads to a shift of the best signals to thinner gold layers. Clavero *et al.* experimentally and theoretically found the highest signal for an Au(20 nm)/Co(2.8 nm)/Au(3 nm) system.¹⁹ Comparing these results with our simulation, we find an optimal Co thickness of approximately 4 nm at comparable gold thicknesses [Fig. 2(a)] verifying the used approach. In a theoretical investigation, González-Díaz *et al.* calculated the MOSPR signal in a three layer system of Au(6 nm)/Co(0–9 nm)/Au(16 nm) and found the best signal for a 6 nm cobalt layer.¹⁸ This is also in good agreement to our simulations [Fig. 2(b)]. Additionally to Clavero *et al.* who optimized the Co thickness for given thicknesses of the Au layers,¹⁹ the present results demonstrate that there is a narrow band of Au thickness combinations for a given Co layer where the δ -signal is maximized.

One approach to further enhance the MOSPR signal is the application of multiple magnetic layers.^{23,24} Therefore in a second set of simulations it has been investigated whether a multilayer system Au/Co/Au/Co/Au gives rise to high δ -signals. Starting from the trilayer system

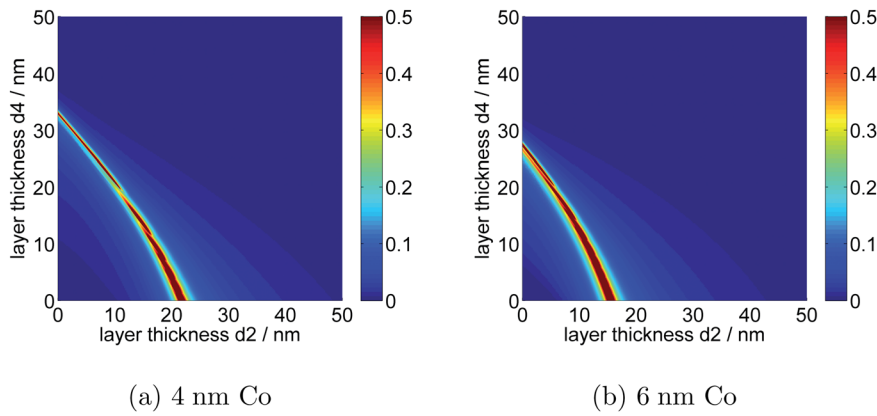


FIG. 2. Influence of the layer thicknesses on the δ -signal with the dielectric air. The maximum of the δ -signal (color scale) is plotted as a function of the two Au layer thicknesses at constant Co thicknesses of (a) 4 nm and (b) 6 nm. d_2 is the thickness of the Au layer situated on top of the glass, d_4 the thickness of the layer facing the dielectric.

Au(10.6 nm)/Co(6 nm)/Au(10 nm) with the maximum δ value of approx. 0.5, an Au layer with increasing thickness (0–5 nm) was introduced into the middle of the cobalt layer. In addition the thickness of the first Co layer has been varied in the range of 0–5 nm leading to the multilayer Au(10.6 nm)/Co(0–5 nm)/Au(0–5 nm)/Co(3 nm)/Au(10 nm). The results are depicted in Fig. 3. They show distinct hot spots of possible thickness combinations leading to high MOSPR signals with δ values up to approx. 35. This demonstrates the potential optimization of MOSPR systems by adding additional magnetic layers.

B. Optimum layers for water

Changing the refractive index of the dielectric of the sandwich system in Fig. 2 from the one of air to the one of water, we observe at first glance a shift of the best MOSPR signal to slightly higher thicknesses of the gold layers [Fig. 4]. It seems to be a phenomenon induced by the ferromagnetic layer. In comparison to the simulations with air it can be seen that the range of Au thickness combinations producing a high MOSPR signal δ is broader in water than using air as dielectric. Furthermore, it changes much less its position upon increasing the cobalt thickness than in air. Both effects show that water as dielectric simplifies the fabrication of multilayer systems with the right thickness suitable for biosensor applications.

C. Biological relevant refractive index changes

For the biosensor not only the dependence of the δ -signal on the layer thicknesses is of interest, but even more so

the dependence of the signal on the refractive index change of the dielectric for a given layer system. For two systems, a pure 50 nm gold layer and an Au/Co/Au trilayer system, simulations with varying refractive index were carried out [Fig. 5]. In order to simulate a realistic biosensor, the layer model from Fig. 4 has been used. In this model, the range of refractive index variation of a 100 nm thick matrix had been chosen to be $n_M = 1.33$ to $n_M = 1.40$, which compares to that of a commercial biosensor [Fig. 1]. The refractive index of the bulk is kept constant ($n_d = 1.33$). The thickness combination of the MOSPR system is Au(10.75 nm)/Co(6 nm)/Au(20.25 nm), an optimal layer combination for water [Fig. 4(b)]. The angle of the minimum reflectivity and the maximum δ -signal are assumed to change linearly with the refractive index. For both systems the linearity holds in good approximation, taking into account, that the change in angle caused by a biological interaction rarely exceeds 2° .²⁵ However, for the considered trilayer the MOSPR signal δ shows a smaller angular dispersion per refractive index change than the gold layer [Fig. 5]. In work of colleagues the enhancement of the sensitivity η has been attributed to both factors that contribute to the sensitivity, the change of signal S per angle A and the change of angle A per refractive index n_d .¹⁴

$$\eta = \frac{\delta S}{\delta n_d} = \frac{\delta S}{\delta A} \frac{\delta A}{\delta n_d}. \quad (3)$$

The current simulations, however, indicate that the derivative of the minimum angle to the refractive index is smaller for the MOSPR signal than for the SPR signal. Hence, this cannot be the source of the enhanced sensitivity.

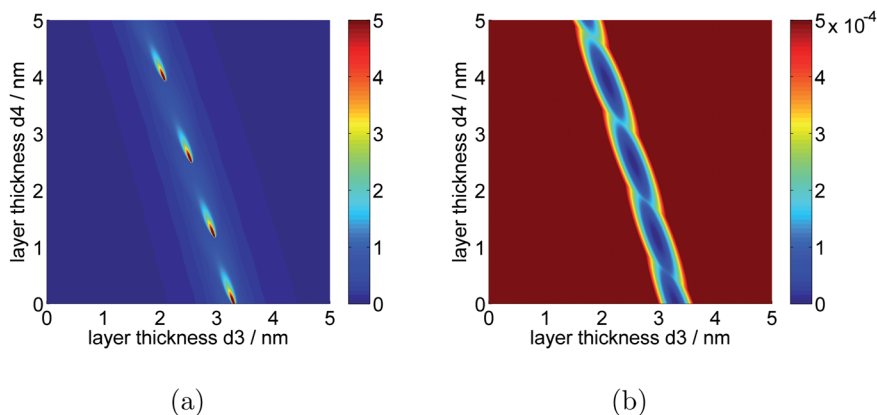


FIG. 3. (a) Height of the maximum δ -signal (color scale), and (b) height of the minimum reflectivity (colour scale) of the multilayer glass/Au(10.6 nm)/Co(0–5 nm)/Au(0–5 nm)/Co(3 nm)/Au(10 nm)/air as functions of the layer thickness d_3 and d_4 .

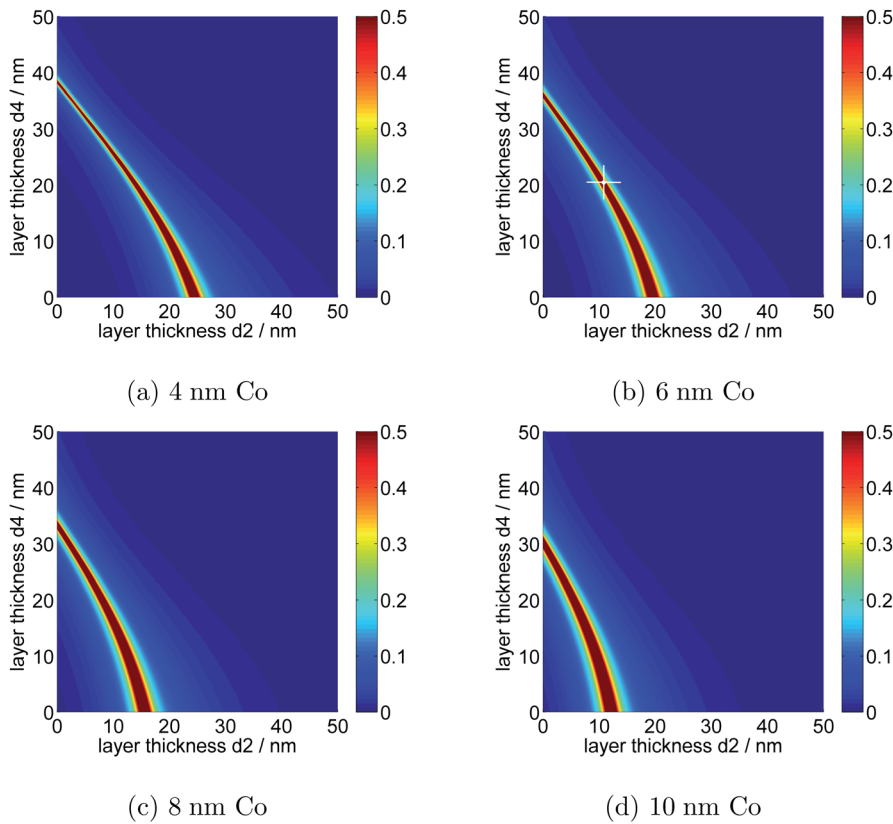


FIG. 4. Influence of the layer thicknesses on the δ -signal with the dielectric water. The maximum of the δ -signal (color scale) is plotted as a function of the two Au layer thicknesses at constant Co thicknesses of (a) 4 nm, (b) 6 nm, (c) 8 nm and (d) 10 nm. d_2 is the thickness of the Au layer situated on top of the glass, d_4 the thickness of the layer facing the dielectric. The white cross in (b) denotes the layer system Au(10.75 nm)/Co(6 nm)/Au(20.25 nm) which has been considered for further investigations.

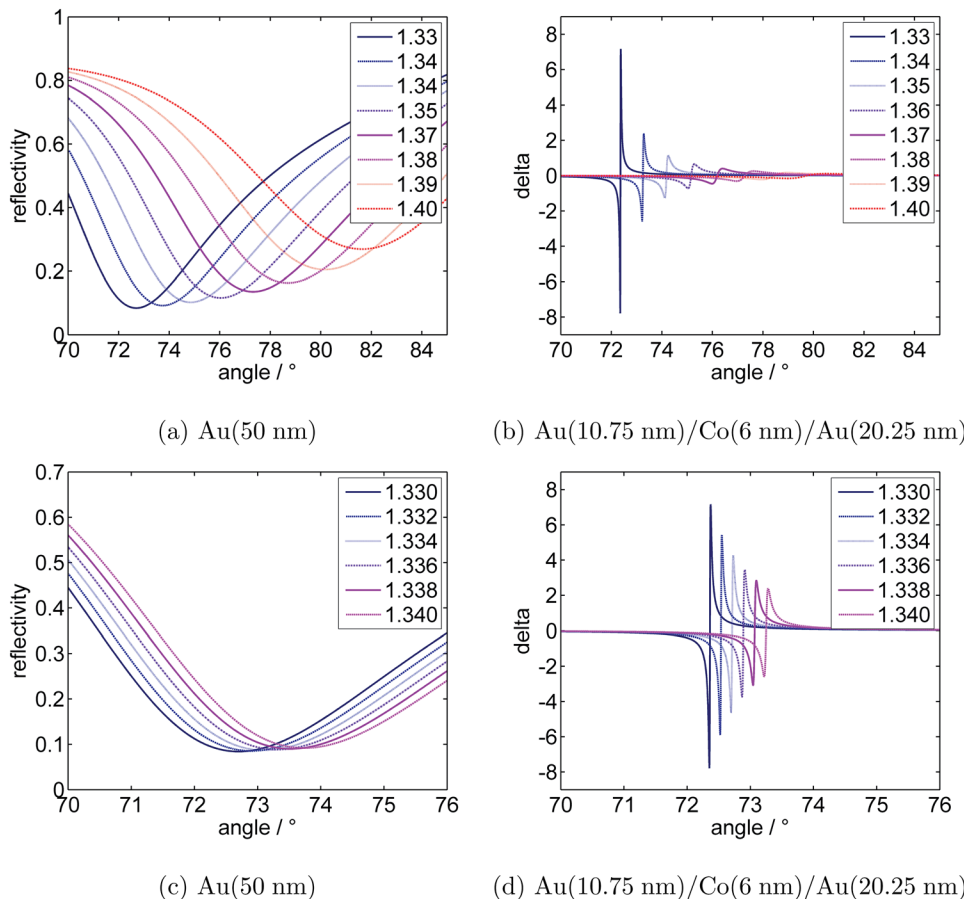


FIG. 5. (a) Reflectivity of a 50 nm gold layer with water as dielectric during a change in refractive index of the 100 nm thick matrix within the range $1.33 \leq n_M \leq 1.40$ with $\Delta n_M = 0.01$ (glass/Au(50 nm)/matrix(100 nm)/water). (b) Change of the δ -signals of a glass/Au(10.75 nm)/Co(6 nm)/Au(20.25 nm)/matrix(100 nm)/water system. (c) Reflectivity curves (glass/Au(50 nm)/matrix(100 nm)/water) and (d) δ -signals (glass/Au(10.75 nm)/Co(6 nm)/Au(20.25 nm)/matrix(100 nm)/water) within the refractive index range $1.33 \leq n_M \leq 1.34$ with $\Delta n_M = 0.002$.

In consequence, the higher sensitivity has to be caused by the large change in signal per angle.

Comparing the amplitude of the two signals for a given refractive index (e.g. $n_M = 1.33$), it can be seen that the SPR signal gives a relatively broad intensity minimum, which creates a small change in signal per angle, whereas the MOSPR signal is much sharper, giving rise to a large change in signal per angle. Besides, we observe, that the magnitude of the δ -signal decays within the chosen refractive index range ($n_M = 1.33 - 1.40$) by a factor > 63 , whereas the minimum reflectivity of the gold layer changes only slightly. For the application of a multilayer system follows, that the range of refractive index change covered by a specific multilayer system, is smaller than the one covered by the gold layer. This might be seen as a disadvantage, but it is not a dead end for the use of magneto-optic multilayer systems as sensor surfaces of a biosensor for two reasons: (1) The goal to enhance the sensitivity in order to see the interactions of small molecules is not affected by the decay of the MOSPR signal, because the refractive index change caused by the specific and unspecific interactions of biomolecules at the sensor surface is very small.²⁵ (2) The full refractive index range might be covered with different multilayer systems. Simulating a series of SPR and MOSPR signals varying the refractive index only in the second decimal place, the advantage of the large change in MOSPR signal per angle for the detection of the refractive index change becomes apparent [Figs. 5(c) and 5(d)]. This is clarified by the fact that in this case ($\Delta n_M = 10^{-2}$) the amplitude of the δ -signal stays within the same order of magnitude [Fig. 5(d)].

IV. CONCLUSIONS

In order to cover the refractive index range of commercial SPR biosensors with an MOSPR set-up, it is essential to adjust the metallic layer system to the refractive index range of the biological system under investigation. Furthermore, we have demonstrated that the sensitivity enhancement is driven by a large change in signal per angle and not by an increased angular dispersion and it has been shown that magnetic multilayer systems with more than one magnetic layer may enhance the sensor sensitivity further. The presented results are useful for the design of an MOSPR sensor and promise high δ -signal values for the dielectric water.

ACKNOWLEDGMENTS

F.W.H. was supported by the EU FP7 collaborative project Affinomics (Contract No.241481).

- ¹J. Homola, *Surface Plasmon Resonance Based Sensors*, Springer Series on Chemical Sensors and Biosensors Vol. 4 (Springer, Berlin, 2006).
- ²E. Kretschmann and H. Raether, *Z. Naturforsch.* **23A**, 2135 (1968).
- ³J. A. De Feijter, J. Benjamins, and F. A. Veer, *Biopolymers* **17**, 1759 (1978).
- ⁴C.-C. Chang, N.-F. Chiu, D. S. Lin, Y. Chu-Su, Y.-H. Liang, and C.-W. Lin, *Anal. Chem.* **82**, 1207 (2010).
- ⁵J. S. Mitchell, Y. Wu, C. J. Cook, and L. Main, *Anal. Biochem.* **343**, 125 (2005).
- ⁶Y. Guo, J. Y. Ye, B. Huang, D. McNerny, T. P. Thomas, J. R. Baker, Jr., and T. B. Norris, *Proc. SPIE* **7553**, 755303 (2010).
- ⁷B. Sepúlveda, A. Calle, L. M. Lechuga, and G. Armelles, *BioWorld Eur.* **1**, 12 (2008).
- ⁸D. Regatos, B. Sepúlveda, D. Fariña, L. G. Carrascosa, and L. M. Lechuga, *Opt. Express* **19**, 8336 (2011).
- ⁹G. Armelles, J. B. González-Díaz, A. García-Martín, J. M. García-Martín, A. Cebollada, M. U. González, S. Acimovic, J. Cesario, R. Quidant, and G. Badenes, *Opt. Express* **16**, 16104 (2008).
- ¹⁰B. Sepúlveda, J. B. González-Díaz, A. García-Martín, L. M. Lechuga, and G. Armelles, *Phys. Rev. Lett.* **104**, 147401 (2010).
- ¹¹J. B. González-Díaz, J. M. García-Martín, A. García-Martín, D. Navas, A. Asenjo, M. Vázquez, M. Hernández-Vélez, and G. Armelles, *Appl. Phys. Lett.* **94**, 263101 (2009).
- ¹²J. B. González-Díaz, B. Sepúlveda, A. García-Martín, and G. Armelles, *Appl. Phys. Lett.* **97**, 043114 (2010).
- ¹³C.-M. Wei, C.-W. Chen, C.-H. Wang, J.-Y. Chen, Y.-C. Chen, and Y.-F. Chen, *Opt. Lett.* **36**, 514 (2011).
- ¹⁴B. Sepúlveda, A. Calle, L. M. Lechuga, and G. Armelles, *Opt. Lett.* **31**, 1085 (2006).
- ¹⁵V. I. Safarov, V. A. Kosobukin, C. Hermann, G. Lampel, J. Peretti, and C. Marlière, *Phys. Rev. Lett.* **73**, 3584 (1994).
- ¹⁶C. Hermann, V. A. Kosobukin, G. Lampel, J. Peretti, V. I. Safarov, and P. Bertrand, *Phys. Rev. B* **64**, 235422 (2001).
- ¹⁷N. Bonod, R. Reinisch, E. Popov, and M. Nevière, *J. Opt. Soc. Am. B* **21**, 791 (2004).
- ¹⁸J. B. González-Díaz, A. García-Martín, G. Armelles, J. M. García-Martín, C. Clavero, A. Cebollada, R. A. Lukaszew, J. R. Skuza, D. P. Kumah, and R. Clarke, *Phys. Rev. B* **76**, 153402 (2007).
- ¹⁹C. Clavero, K. Yang, J. R. Skuza, and R. A. Lukaszew, *Opt. Express* **18**, 7743 (2010).
- ²⁰J. Zak, E. R. Moog, C. Liu, and S. D. Bader, *J. Appl. Phys.* **68**, 4203 (1990).
- ²¹J. Zak, E. R. Moog, C. Liu, and S. D. Bader, *Phys. Rev. B* **43**, 6423 (1991).
- ²²Z. Q. Qiu and S. D. Bader, *Rev. Sci. Instrum.* **71**, 1243 (2000).
- ²³T. Katayama, Y. Suzuki, H. Awano, Y. Nishihara, and N. Koshizuka, *Phys. Rev. Lett.* **60**, 1426 (1988).
- ²⁴K. Sato in *Magnetic Multilayers*, edited by L. H. Bennett and R. E. Watson (World Scientific, Singapore, 1994), p. 277–297.
- ²⁵B. Liedberg, C. Nylander, and I. Lunström, *Sens. Actuators* **4**, 299 (1983).